Proceedings of the 21st ICSMGE, Vienna, Austria, 14 – 19 June 2026. Pistrol, Adam & Schweiger (eds.)
Published by: ÖGG, Austrian Society for Geomechanics, Salzburg, Austria, ISBN 978-3-9503898-4-5
https://doi.org/10.53243/ICSMGE2026-1483

Quality control of strain dissipating trenches for the mitigation of soil cracks

Moisés Juárez-Camarena, Cinthya Cervantes-Barranco, Gabriel Auvinet, Edgar Méndez-Sánchez
Instituto de Ingeniería, UNAM, Mexico, mjuarezc@iingen.unam.mx

Sergio Martínez-Galván
SEPI, ESIA, UZ, IPN, and Instituto de Ingeniería, UNAM, Mexico

ABSTRACT Differential settlements between subsiding lacustrine clays and firm soils originate large cracks in the soil of southern Mexico City. Strain dissipating trenches have been designed to mitigate damage induced by soil fissuring. In this paper, the results of a quality control campaign performed during the construction of these trenches are presented. The research is based on results obtained using the Lightweight Dynamic Cone Penetrometer of Variable Energy (PANDA), soil mechanics tests, as well as field observations at the treated sites. With these results it has been possible to define a complete methodology for the construction of strain dissipating trenches.

KEYWORDS: Valley of Mexico, subsidence, cracks, damage, pavement, deformation dissipating trenches, PANDA.

1 INTRODUCTION

Land subsidence caused by deep-well pumping has affected very large Asian cities, including Tokyo, Osaka, Shanghai, Taipei, Bangkok, Jakarta, Calcutta, Manila, and Hanoi (Akagi, 1979; Lui, 1991, Yong *et al.,* 1995), where severe impacts were eventually controlled through groundwater-management programs and the development of surface-water supply systems. Similarly, the Valley of Mexico experiences significant regional subsidence due to deep-aquifer pumping, generating differential settlements that induce tensile and shear stresses within the ground. As a result, the most severe soil cracks in the region are a direct manifestation of this ongoing subsidence process.

The problem of soil cracking constitutes an important risk factor that must be evaluated to define the protection and coexistence measures required to prevent or at least mitigate the damage that may be caused to buildings, pavements and hydraulic installations. In Mexico City, a considerable number of cracks in the soil have been treated using shear strain dissipative trenches (Auvinet *et al*., 2019). Those trenches are excavated along the path of the cracks and filled with clean sand placed in compacted layers. The presence of sand prevents the upward transmission of cracks to the surface and reduces damage to the pavement.

To evaluate the degree of compaction of the sand material and calibrate the quality control criteria, a test program was defined with two specific objectives: first, determine the optimal thickness of the layer for the accommodation of the granular material; second, establish the number of passes necessary with a given equipment to achieve an optimal degree of compaction.

2 MEXICO VALLEY SUBSOIL

2.1 *Stratigraphy*

The geotechnical characteristics of the area of interest (southeast of Mexico City) are known in certain detail from the numerous geotechnical borings performed for different constructions in the area, especially Lines “12” and “A” of the subway system. This information has been documented in different thesis works (Flores-Tapia, 2000; Aguilar-Ortega, 2001; Morales de la Cruz, 2001; Barranco-Eyssautier, 2016) and summarized in Auvinet *et al*. (2017).

Figure 1 shows the geotechnical zoning of the southern area of Mexico City, as defined in the Complementary Technical Standards for Design and Construction of Foundations for Mexico City (NTCDCC) published in 2023. The areas corresponding to zones I (Lomas: hills), II (Transition) and III (Lake) are indicated.

At the Colonia Del Mar site, borings SM-01, SM-02 y SM-03 with maximum exploration depth of 74.8, 83.0 and 83.0m, respectively, were performed, as well as three electric cone tests with pore pressure measurement CPTu-01, CPTu-02 and CPTu-03, with maximum depth of 57.78, 63.0 and 39.28 m, respectively. Figure 2 shows the location of borings.

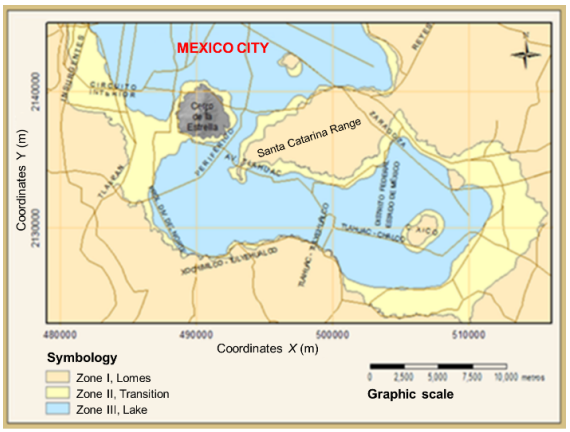

Figure 1. Geotechnical zoning of Mexico City southern area (NTCDCC, 2017).

Figure 2. Location of borings, *Colonia del Mar* site.

In Figure 3, a cross section of the subsoil at this site is presented. A difference of approximately 25m in clay thickness can be observed between the deep level benchmark (BNP) and boring SM-01. The thickness of clay increases towards the southwest. Likewise, the clay thickness between wells SM-01

and SM-02 is approximately constant but between borings SM-02 and SM-03 a difference of 32m is observed due to the presence of a buried basaltic flow.

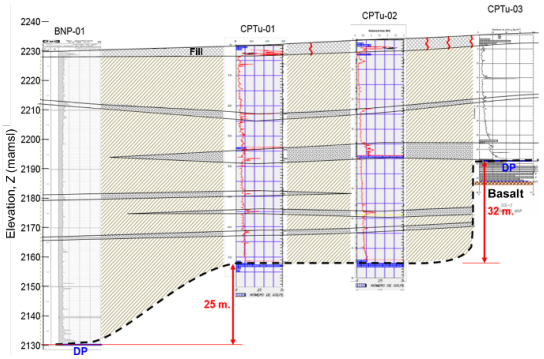

Figure 3. Cross section of the subsoil, *Colonia del Mar* site.

2.2 *Regional subsidence*

Regional subsidence in the lacustrine soil and fluvial-lacustrine areas of the Valley of Mexico is a natural phenomenon caused by the pumping of water from deep aquifers. Regional subsidence affects the performance of buildings and causes periodic flooding in certain areas during the rainy season.

Figure 4 shows a map of regional subsidence rate in the lake area of the Mexico valley is presented (Juárez *et al*., 2021).

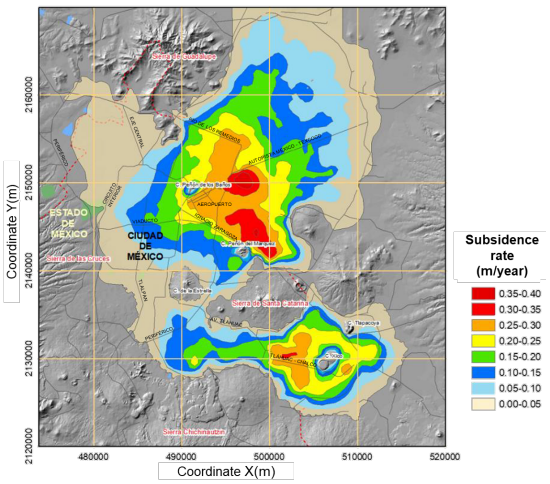

Figure 4. Subsidence rate map of Mexico valley (Juárez *et al*., 2021).

The subsidence rate map of Mexico valley was prepared from elevation data measured by the Mexico City Water System (SACMEX) and other government agencies, during the 1983 to 2017 period, through topographic surveys of surface references. In this map, it can be observed that at some sites the rate of subsidence reaches almost 35 cm/year.

2.3 *Soil cracking*

Soil cracking in the Valley of Mexico has various causes, including the contraction of lacustrine clays due to drying, the existence of tensile and shear stresses associated with the weight of buildings, hydraulic fracturing in flooded areas, seismic movements, etc. However, the most significant and destructive cracks are a direct consequence of the differential settlements induced by regional subsidence occurring in the Valley of Mexico due to the pumping of water from deeper strata.

As subsidence increases, ground cracking, which previously occurred only in the dry basin of Lake Texcoco, has become more prominent in the transition zone, as a result of differential settlements between soft and firm soils, resulting in damage to buildings and urban facilities. Figure 5 shows one of the areas where the cracking phenomenon is most prevalent (on the outskirts of the Santa Catarina range).

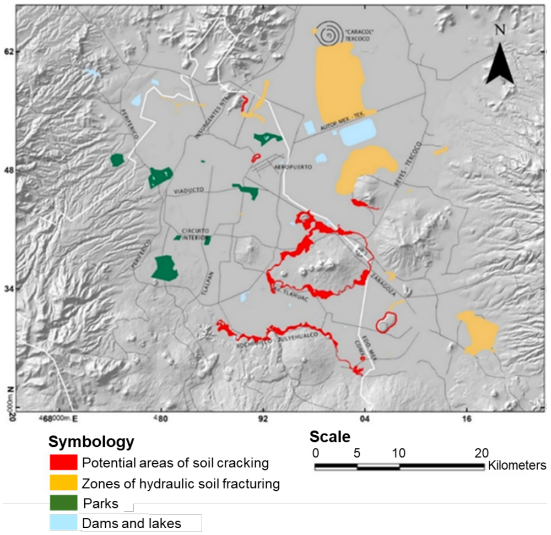

Figure 5. Map of potential soil cracking zones.

2.4 *Cracking mechanism*

Deep geotechnical exploration confirms that soil cracking in the area results from the abrupt variation in lacustrine clay thickness across the transition between soft and firm materials. Under these conditions, clay consolidation produces pronounced differential settlements that generate tensile and shear stresses, leading to cracking. This mechanism can be reproduced by finite element analyses and corresponds to the mechanism defined as Type II by Auvinet *et al*. (2017). The condition of Figure 6 (*Colonia Del Mar*) is representative of those existing in the area

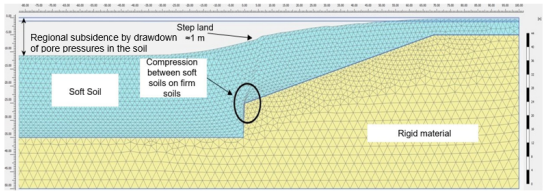

a) Deformed mesh

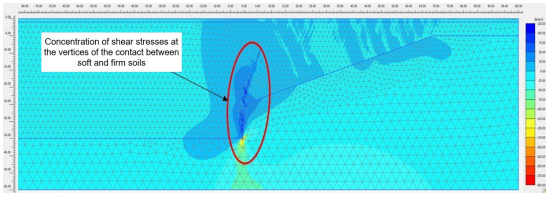

b) Shear stresses

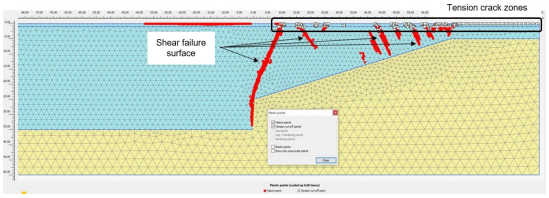

c) Puntos plásticos y de tensión

Figure 6. Numerical modeling of the consolidation of a clayey layer of variable thickness.

In the same figure, the plastic points (represented in red) are located along certain zones defining trajectories that propagate from the bottom to the surface. These trajectories

represent planes where the resistance to shear stress is null, under this situation the planes can be separated and form cracks.

The generation and propagation of cracking has also been modelled using fracture mechanics (Pineda and Auvinet, 2021).

On the other hand, the seismic behavior of the cracked soil has been analyzed for the conditions prevailing at this same site (Martínez *et al*., 2021). It was concluded that ground acceleration is strongly amplified by the presence of cracks and that permanent displacements in the cracks such as those observed on Figure 7 can appear during earthquakes.

3 DAMAGE CAUSED BY SOIL CRACKS

Ground cracks can cause considerable damage to pavements, buildings, and hydraulic installations. Figure 7 shows an example of the damage caused to pavements by cracks in the soil of a site located at the foot of the Santa Catarina range, southeast of Mexico City downtown.

Figure 7. Damages caused to pavements by soil cracks.

In Figure 8, some damages to a construction due to soil cracks are shown.

Figure 8. Damage to a house caused by the development of cracking, San Sebastián Tecoloxtitila, Iztapalapa Municipality (SCER, 2024).

4 STRAIN DISSIPATING TRENCHES FOR MITIGATION OF DAMAGE TO PAVEMENTS

In the past, different methods have been used to mitigate soil cracking, such as grout injection (Yong *et al*., 1995)., soil replacement, geosynthetics, and pavement reinforcement. Grout injection tends to induce crack propagation. Geosynthetics increase tension resistance of soil but their performance decreases for large settlements (Zhang *et al*., 2009; Pérez-Rea *et al*., 2018).

To mitigate this problem in Mexico City, II-UNAM has proposed using "angular strain dissipation trenches". This solution consists of a trapezoidal excavation along the crack filled with clean sand. This granular material cannot transmit tensile stresses and dissipates unitary shear strains within the surficial soil, avoiding direct damage to the pavement (Auvinet *et al*., 2019). The dimensions of strain dissipation trenches are adapted to the different conditions encountered on each site, based on analyses performed using the discrete element method (Auvinet, 2019) (Figure 9). According to current regulations (GOBCDMX, 2023), the maximum allowable slope for vehicle ramps is $\delta z/L=0.15$. An appropriate depth, h, should thus be selected for the granular trench to maintain the surface slope below the maximum allowable value for an acceptable period. Subsequent maintenance work will be required to level the surface. In important roads, deeper trenches should be considered. In Figure 10, the procedure for building a strain dissipation trench is shown.

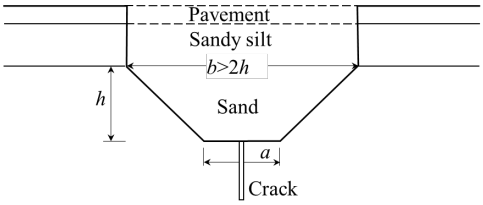

Figure 9. Conceptual design of a strain dissipation trench.

a) Cutting of asphalt pavement on road.

b) Excavation for strain dissipation trench.

c) Placement of granular material fill and compaction.

d) Preparation of pavement base for placement of asphalt.

Figure 10. Construction procedure of a strain dissipation trench for roads (Risk Assessment Center, Iztapalapa).

This solution has been applied to more than 1700 sites in the Iztapalapa precinct as part of a wide program named "Urban Acupuncture" for mitigation of cracks. The results have been

satisfactory and no or only light maintenance has been required in the first operation years.

5 QUALITY CONTROL PROCEDURE

In an initial stage, sand trenches were built without following a specific and detailed construction procedure. In most cases, the fill material was placed in layers with different thickness, as well as using different compaction techniques and equipment. Clearly these variations can impact directly the performance and durability of the sand trenches. In a small number of cases the trenches presented damage, which shows that some layers of sand were not compacted correctly. Therefore, it was necessary to build some experimental dissipating trenches following different methodologies, with the aim of defining a specific procedure to specify and control the quality of the construction of these strain dissipating trenches. The methodology used for this study is described below.

5.1 *Material for the fill*

For this study, sand samples were obtained from 10 material banks. The sample materials were analyzed to obtain particle size distributions; typical results are presented in Figure 11. The fines content was found to vary depending on the material bank.

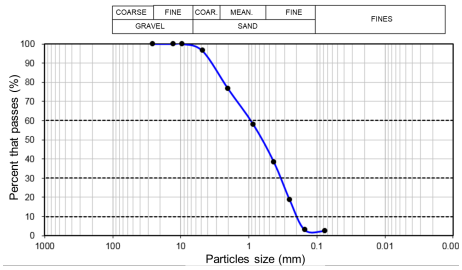

$D_{10} = 0.20$ $D_{av} = 5.70$ $Gravel = 3.7\%$
$D_{30} = 0.33$ $C_u = 4.8$ $Sand = 94.0\%$
$D_{60} = 0.95$ $C_c = 0.6$ $Fines = 2.3\%$

Figure 11. Grain size distribution of the granular material used.

5.2 *Compaction equipment*

For granular materials (sand), a vibratory compaction process reduces internal friction due to compactor pressure, which improves particle coupling, reduces the possibility of void formation, and counteracts capillary tension forces. Therefore, for compact the granular soil in this work, a manual push ram Husqvarna, model LT 6005, weighing 69 kg, with a base width of 280 mm/11 in, engine power of 3600 rpm, and vibration frequency of 11.9/714 Hz (Figure 12) was used.

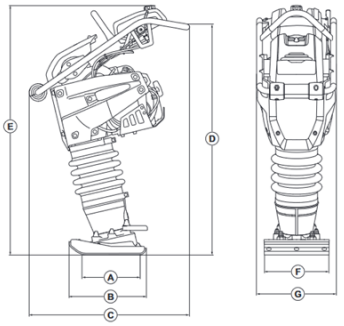

A	Contact area of the base of the manual push ram, m^2/square feet	0.053/0.57; 0.065/0.70
B	Length of footing foundation of the manual push ram, mm/inch.	330/13
C	Length, mm/inch.	726/28.6
D	Handle height, mm/inch	935/36.8

Figure 12. Manual push ram Husqvarna 6005 diagram.

5.3 *PANDA equipment*

The PANDA equipment (Assisted Digital Autonomous Penetrometer) is a lightweight dynamic penetrometer of variable energy. This equipment was developed by researchers of the Geotechnical Group in the Blaise Pascal University, France in conjunction with the research and development department of the French company Sol-Solution. Initially it was used as a technological tool for soil recognition up to average depths of 7 m with a maximum particle size of 2". Later, in 2000, this equipment was standardized (XP P94-105 Standard) to extend its application as an effective method for controlling the soil compaction in embankments, roads and dams (Espinace *et al*., 2013).

The PANDA equipment basic operating principle consists in thrust by blows, using a standard 2 kg hammer, a set of 14 mm diameter bars, equipped with a 2 or 4 cm^2 metal conical tip (Figure 13).

For each hammer blow, the penetration achieved is continuously recorded. The resistance of the tip in the soil associated with the transmitted energy is calculated using the Dutch thrust equation (1) proposed by Caquot (1956). This equation shows that the tip resistance depends on the energy applied by each blow to the hammer, the penetration achieved, the mass of the hammer and the mass of the bars train.

$$q_d = \left(\frac{1}{A_c}\right) * \left(\frac{E}{e}\right) * \left(\frac{M}{M+P}\right) \quad (1)$$

Where:

A_c, tip area (m^2)
E, applied energy [J]
e, penetration of the tip into the soil each hammer blow (m)
M, hammer mass used (kg)
P, mass of bar train and hitting head (kg)

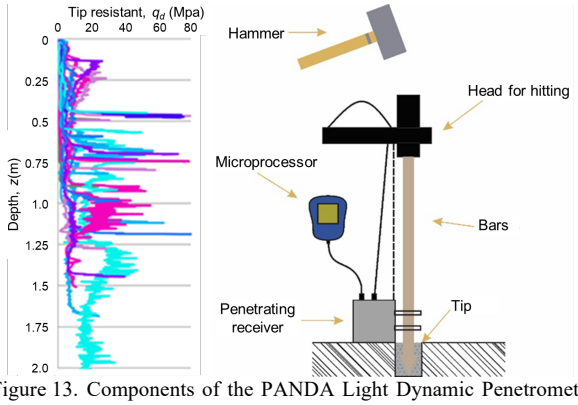

Figure 13. Components of the PANDA Light Dynamic Penetrometer (Modified from Villavicencio, 2007).

5.4 *Determination of the resistance of the fill varying sand layers thickness*

To determine the optimal layer thickness, four experimental sand trenches were built at a uniform depth of 0.80 m, each with a different layer thickness. The sand used as fill was previously sampled and analyzed in the laboratory to verify compliance with the required particle-size distribution and fines content.

In all cases, the same compaction technique and equipment were used.

After concluding construction of the sand trenches, the resistance of the fill was measured using the PANDA equipment.

Figure 14 shows that the optimal resistance profile corresponds to the sand trench constructed with 20 cm thick layers. This thickness provides the greatest resistance and also provides a virtually uniform resistance distribution throughout

the depth of the experimental sand trench. For practical applications, it ensures that the granular material will be compacted uniformly, reducing potential variations in density and resistance of the sand.

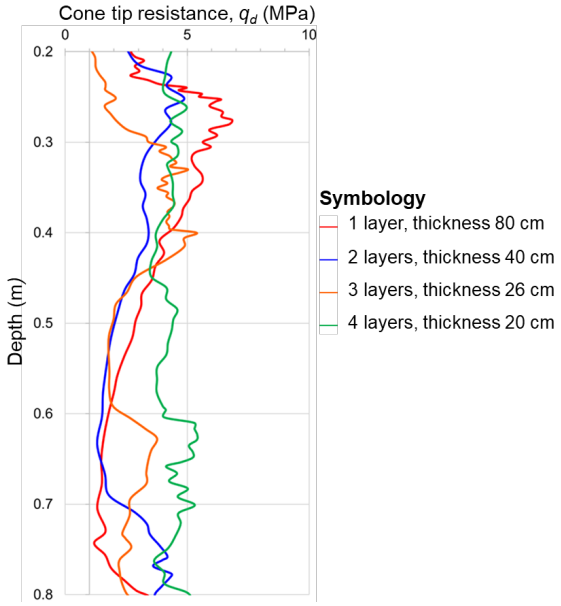

Figure 14. Resistance profiles obtained with PANDA equipment in each experimental trench, varying the layers thickness.

5.5 *Determination of the resistance of the sand fill by varying the number of passes with the compaction equipment*

To determine the number of passes required using the compaction equipment in a sand trench, 40 experimental trenches were constructed with sand layers 20 cm thick; in each sand trench the number of passes was different.

To compact the sand layers, the vibratory compaction equipment previously described (Husqvarna LT 6005 hand-held rammer) was used. Figure 15 presents the resistance profiles obtained with the PANDA dynamic penetrometer for eight experimental sand trenches, showing only the most representative profiles for interpretation.

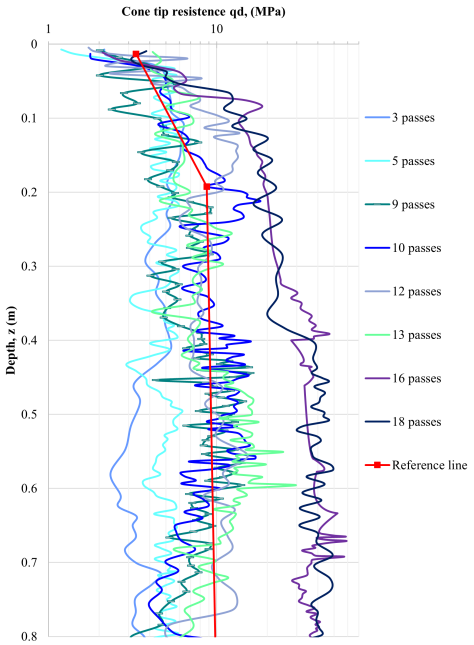

Figure 15. Resistance tip profiles obtained with PANDA equipment in each experimental trench, varying the number of passes.

In Figure 15, it can be observed that the tip resistance profile obtained with 10 passes of the compaction equipment shows the highest and more uniform resistance along the depth. Also, in the same figure, the line represents the mean of tip resistance profile (9MPa), which will be used as reference for compaction quality control.

5.6 *Calibration chart for compaction control*

Based on the results obtained from the experimental trenches, a reference line can be defined as the mean resistance corresponding to 9 MPa (10 passes; Figure 16). Considering the inherent variability of the construction process, the standard deviation of the data was calculated to estimate the range within which the strength could fluctuate with respect to the mean. The strength tolerance limits were established as a minimum of 4 MPa (undercompacted) and a maximum of 14 MPa (overcompacted).

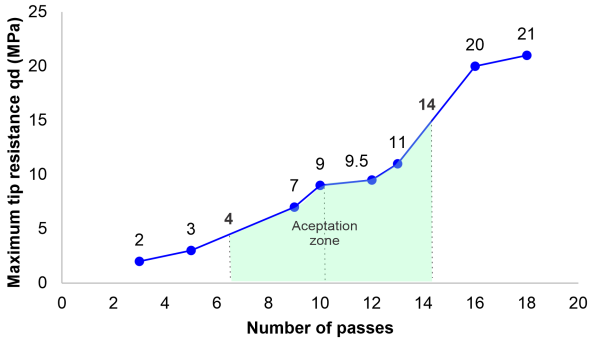

Figure 16. Effect of the number of passes of the compaction tool and maximum (q_d) resistance recorded in the profile.

This tolerance zone was defined as the acceptance zone of the spatial variations in the compacted granular material.

The acceptance tolerance considers the geometry of the excavation, the thickness of sand layers and the influence of the applied compaction energy, it also considers the noise in the PANDA equipment signal, generated during the test.

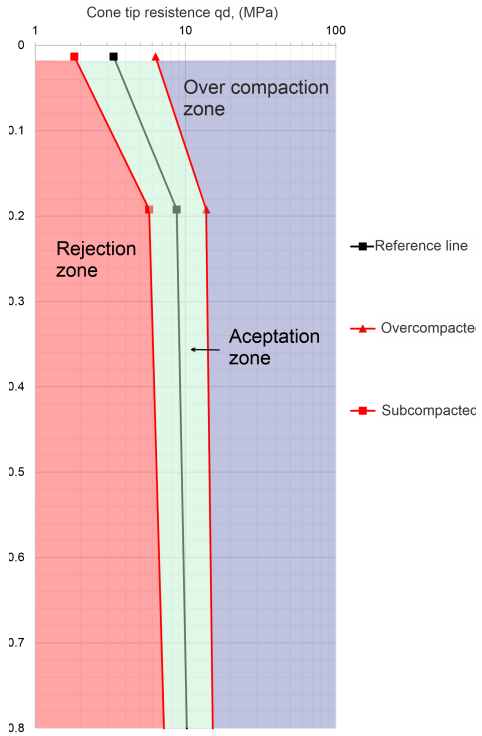

Figure 17. Chart for compaction quality control in strain dissipating sand trenches.

This calibration chart will be used as reference for the quality compaction control. Thus, it will be possible to ensure that the granular material deposited in the sand trenches achieves the desired resistance properties during compaction process. As an example, Figure 17 shows that the profile resistant line for 10 passes enters the rejection zone in the 0.6 - 0.8m stretch, therefore the compaction is not accepted, because the resistance is less than the value corresponding to the acceptance line.

6 METHODOLOGY TO EVALUATE THE QUALITY CONTROL

Based on the results of this research, the following methodology is defined for the construction of deformation dissipating trenches, as follow:

1. Excavation of a trench with trapezoidal geometry (Figure 9).
2. Supply the sand for filling and perform the corresponding tests to verify compliance with the granulometric specifications.
3. Build the fill in 10 cm thick layers and compact them with a hand pushed ram equipment (Husqvarna LT 6005 or similar) applying 10 passes per layer
4. Performs some tests with PANDA equipment in sites randomly selected.
5. Plot the profile tip resistance on the calibration chart to determine if the measured resistance is within or out from the acceptance zone.

7 CONCLUSIONS

The results of this research allow concluding that, for optimal compaction of the sand fill for strain-dissipating trenches, sand with a fines content of <15% should be used, arranged in 20-cm-thick layers and compacted with 10 passes of the vibratory equipment. Recently, 74 cracks have been mitigated applying this technique. The evidences show that the cracks improved by this technique have greater durability over time than any other mitigated technique previously used. This trench dissipation strain technique offering a cost-effective and rapidly deployable alternative in urban settings.

8 ACKNOWLEDGEMENTS

The authors thank *Instituto para la Seguridad de las Construcciones del Gobierno de la Ciudad de México* (Institute for Construction Safety of Mexico City, GOBCDMX) for its sponsorship of this research. Likewise, to the Iztapalapa municipality office for its sponsorship of the experimental strain dissipating trenches.

9 REFERENCES

Akagi, T. 1979. Some land subsidence experiences in Japan and their Thailand. Geotechnical relevance to subsidence in Bangkok, Engineering Journal, Vol. 10, No. 1, pp. 1-48.

Auvinet, G., Méndez, E. y Juárez, M. 2017. *El subsuelo de la Ciudad de México/Subsoil of Mexico City, Vol. 3*, published on the occasion of the 60th anniversary of the founding of Instituto de Ingeniería, UNAM. ISBN Vol. 3 978-607-02-8198. Mexico.

Auvinet, G., Sánchez-Guzmán, J. y Pineda, A.M., 2019, "*Mitigación de daños ocasionados por grietas en el suelo*", Revista Ingeniería, Investigación y Tecnología, Volumen XX (Número 4) octubre-diciembre 2019 1-8, ISSN 2594-0732, FI-UNAM, Mexico

Auvinet, G. y Sánchez-Guzmán, J. 2023. *Estructura y micromecánica de medios granulares/Fabric and Micromechanics of Granular Media*, bilingual volume, joint publication by II-UNAM and SMIG, Mexico, 554 p., ISBN 978-607-59398-3-4. Mexico.

Espinace R. *et al*. 2013. The PANDA equipment as a learning tool in geotechnics. Procedings of *IV Congreso Panamericano de enseñanza y aprendizaje de Ingeniería Geotécnia*.

II-UNAM. 2019. *Modelado numérico del agrietamiento del suelo y de algunas medidas de mitigación. Aplicación a la problemática de las alcaldías Iztapalapa, Tláhuac, Xochimilco y Milpa Alta*, Collaboration agreement between II-UNAM and Secretariat of Education, Science, Technology and Innovation (SECTEI) of This trench dissipation strain technique offering a cost-effective and rapidly deployable alternative in urban settings.Mexico City, Mexico.

Juárez Camarena, M., Román Rosario, H., Auvinet Guichard, G., and Méndez Sánchez, E. 2021. Contribución a la actualización del mapa de hundimiento regional para el Valle de México. XXX Reunión Nacional de Ingeniería Geotécnica. México.

Lui, Tiezhu, 1991. Land subsidence in Shanghai. In Shanghai Land Shanghai, China, October, pp. 1-14.

Pérez-Rea, M., Santoyo, E., & Ovando, E. (2018). Differential settlement effects on geotechnical structures in Mexico City clays. *Revista Ingeniería Sísmica*, 98, 45–62.

Subsidence Volume, Bureau of Geology and Mineral Resources of

NTC-DCC. 2023. Normas Técnicas Complementarias para Diseño y Construcción de Cimentaciones, *Gaceta Oficial de la Ciudad de México, december 15th*, Mexico.

Martínez, S., Auvinet, G., and Juárez, M. 2021. Análisis numérico del comportamiento sísmico del subsuelo en presencia de grietas. Pocedings of *XXX Reunión Nacional de Ingeniería Geotécnica*.

Pineda A.R. y Auvinet G. 2021. Generación de grietas y crecimiento de escarpes en suelos agrietados de la Ciudad de México, Proceedings of *XXX Reunión Nacional de Ingeniería Geotécnica*. Mexico.

Sub Office Direction Risk Assessment Center (SCER), Iztapalapa Municipality. 2024. Photographs provided personally.

Villavicencio, G., Bacconnet, C., Breul, P., Boissier, D. y Espinace, R. 2007. *Probabilistic evaluation of the parameters governing the stability of the tailing dams. 1rst International Conference on Information Technology in Geo-Engineering (ICITG)*. Shanghaï, 16-17. September, pp. 108-116. China.

Yong, R.N., Maathuis, H. and Turcott, E., 1995, Groundwater abstraction-induced land subsidence prediction: Bangkok and Jakara case studies, Proceedings of the Fifth International Symposium on Land Subsidence, FISOLS-95. The Hague, Netherlands.

Zhang, L., Zhao, M., & Chen, R. (2009). Performance of geosynthetics under differential settlement: A case study in Eastern China. *Geotextiles and Geomembranes*, 27(3), 179–190.